Structure and dynamics of the excited CH–chromophore in $(CF_3)_3CH$

J. E. Baggott,[a] M. -C. Chuang, and R. N. Zare

Department of Chemistry, Stanford University, Stanford, California 94305

H. R. Dübal and M. Quack

Laboratorium für Physikalische Chemie der ETH, CH 8092 Zürich, Switzerland

The absorption spectra of gaseous $(CF_3)_3CH$ (1,1,1,3,3,3-hexafluoro, 2-trifluoromethyl propane) were recorded in the IR between 800 and 12 000 cm^{-1} by high resolution interferometric Fourier transform techniques and in the visible from 12 000 to 17 000 cm^{-1} by laser photoacoustic spectroscopy. Instead of single bands in the CH overtone region, complex multiplet structures were observed. Thirty-nine bands were assigned as arising from the interacting CH-stretching and CH-bending manifolds, which account for most of the absorption in the overtone region. The results can be understood quantitatively with an effective, tridiagonal many-level Fermi resonance Hamiltonian. Close agreement is obtained for the positions and intensities of the observed spectral features using only seven spectroscopic parameters. The experimental and theoretical results are summarized in Tables II, III, and IV. The Hamiltonian can be used to calculate and understand the time-dependent redistribution of vibrational energy between the coupled CH-stretching and CH-bending vibrations. The role of broad vibrational band shapes and the possible exponential decay of CH excitation into a background of states from low-frequency vibrations is discussed.

I. INTRODUCTION

Understanding intramolecular vibrational energy transfer in large polyatomic molecules is one of the most important challenges in chemical reaction dynamics (a good survey of various aspects of the problem can be found in a recent Faraday Discussion[1]). Vibrational redistribution, often including rotation, has profound effects in molecular spectra,[2] is essential for the mechanism of unimolecular reactions with thermal,[3] photochemical,[4] and IR–photochemical[5] initiation, and is of crucial importance in assessing the possibilities of mode selective chemistry.[6] Some time ago, it was realized[7] that the isolated CH chromophore in an environment of otherwise heavy atoms may serve as a model system for investigating vibrational redistribution through the study of fundamental and overtone absorption spectra. In saturated (alkyl) compounds it has been found that there is a universal anharmonic interaction which tightly couples the CH stretching and bending motions.[7-10] A similar coupling has also been proposed by Sibert, Reinhardt, and Hynes[11] to account for the vibrational bandwidths in the CH–overtone spectra of benzene and related compounds.[12] An appropriate effective Hamiltonian could be established and proved to provide accurate fits and unambiguous assignments in the case of CF_3H[8] and CD_3H,[9] where the analysis can be carried out by means of the resolved rotational structure of the vibrational band systems.

For large polyatomic molecules such as $(CF_3)_3CH$ the rotational line structure of the vibrational absorption cannot be resolved under ordinary conditions, due to the very dense, homogeneous and inhomogeneous vibrational structure with average *vibrational* line densities already exceeding $10^6/cm^{-1}$ in this molecule.[7,10] The vibrational bands at room temperature and even at 200 K are therefore broad and essentially continuous even at Doppler limited resolutions, showing only sometimes a few residual features arising from rotational structure in the band envelopes. A simple local[13] or normal stretching mode model for the CH-overtone spectra would thus predict individual broad bands at the positions expected from a single anharmonic CH oscillator. In contrast to this, the CH stretching–bending Hamiltonian predicts nontrivial vibrational coarse structure for each overtone band, which contains significant information about the CH stretching–bending redistribution.[14] This allows for an adequate test of the assignments even without rotational line structure being measurable. It was therefore decided to cover the whole relevant spectral range from 1000 to 17000 cm^{-1} for $(CF_3)_3CH$, using a combination of FTIR[8] and laser photoacoustic spectroscopy techniques.[6,15]

For our experiments $(CF_3)_3CH$ is a fairly ideal molecule, being a symmetric top with a well defined environment for the CH chromophore and correspondingly well defined polarization of the overtone transitions. It is chemically inert and stable. In spite of its substantial molecular weight it has a high vapor pressure (170 kPa≈1.7 atm at 300 K). Apart from the previous investigations related to the present work,[7,10] there is relatively little work available on $(CF_3)_3CH$ (tristrifluoromethylmethane). The molecular structure has been studied by electron diffraction.[16] Bürger and Pawelke[17] have obtained vibrational spectra in the fundamental region and have provided a normal coordinate analysis. The necessary ground work is available concerning the temperature dependence of the rotational and vibrational band shape of the CH-fundamental transition.[10,18] In the present paper we report the results of our investigations of the CH-overtone transitions, which provide a rather satisfactory understanding of the short time dynamics of the isolated CH chromophore in a large polyatomic molecule.

II. EXPERIMENTAL

The synthesis of (CF$_3$)$_3$CH has been reported before.[17,19] For our experiments, the compound was prepared by addition of HF to perfluoroisobutene.[7] After purification and drying, it did not show any sizeable impurities. It easily dissolves air and was therefore thoroughly degassed by freeze–pump–thaw cycles, whenever this appeared to be necessary. In the long path spectra, some absorption from small amounts of water are usually visible, but these are quantitatively unimportant and useful in practice for calibration purposes.

The IR spectra between 800 and 12 000 cm^{-1} have been measured with the BOMEM DA.002 interferometric Fourier transform spectrometer system of the Zürich group. Details of the techniques have been described elsewhere.[8] The system allows for a maximum apodized resolution of 0.004 cm^{-1} and a similar absolute wave number accuracy is achieved by reference to a single mode He–Ne laser which is used for measuring the mirror displacement in the Michelson interferometer. Because of the broad bands observed for (CF$_3$)$_3$CH this resolution and accuracy was actually not necessary and was not used in practice. The FTIR data given in the Results section are all intrinsically accurate to within much less than the uncertainties of the determination of the centers of broad bands (the latter uncertainties amount to values between 0.1 and a few cm^{-1}, depending upon the bands considered). Single- and multipass cells with optical path lengths up to somewhat more than 20 m were used. At 10^6 Pa pressure these path lengths allow us to record spectra in the CH-overtone region up to about 12 000 cm^{-1}. Beyond this range the more sensitive laser photoacoustic spectroscopy had to be used.

The overtone spectra in the visible region (12 000 to 17 000 cm^{-1}) were measured using intracavity cw dye laser techniques which have been described in detail in previous publications of the Stanford group.[6,13] A sample cell for the vapor, complete with microphone (Brüel and Kjaer model 4144) was placed inside the cavity of a home built linear dye laser operating with the dyes in ethylene glycol solution as summarized in Table I. Spectra Physics models 171-01 Kr$^+$ and 165-03 Ar$^+$ ion lasers were used as pump sources. The ion laser pump beam was modulated by mechanical chopping at frequencies in the range 500–700 Hz and the microphone signals were processed by a lock-in amplifier (PAR

model 124 A). The wavelength regions accessible using LD 700 and rhodamine 6G dyes were calibrated by recording optogalvanic signals from a hollow cathode (Westinghouse Corp.) filled with neon. A neon hollow cathode lamp supplied by Perkin–Elmer was used for the wavelength region covered by DCM. The wavelength tuning was achieved by rotating a (motor-driven) two-plate birefringent filter (Coherent) placed at Brewster's angle inside the dye laser cavity. This was found to result in slight nonlinearity in the wavelength scales, and, as a consequence, experimental values for the position of the absorption maxima of the high overtones are expected to be accurate to within $\pm$ 8 cm^{-1}. This is still adequate for the very broad bands observed in this spectral range. The intracavity laser power was monitored using light reflected from one of the Brewster-angle windows of the sample cell into the sensor head of a NRC model 815 power meter; the resulting signal was processed by a second lock-in amplifier. Normalization of the photoacoustic spectra was achieved by ratioing the output signals from both lock-in amplifiers (PAR model 193 ratiometer). The pressures of (CF$_3$)$_3$CH used were in the range 2$\times$10^4–4$\times$10^4 Pa. Finally, all data were stored, processed, and transferred in digital form.

III. RESULTS AND DISCUSSION

A. Survey of multiple Fermi resonance structures in the overtone spectra

Figure 1 shows a survey spectrum of (CF$_3$)$_3$CH (l = 22.5 m, P = 4.74$\times$10^4 Pa) for the region from 4000 cm^{-1} to 9000 cm^{-1}, which includes the first CH-stretching overtone expected near 5900 cm^{-1} and the second overtone expected near 8600 cm^{-1}. Instead of one overtone band, multiplets of bands are observed, because the tridiagonal Fermi resonance couples CH-stretching (quantum number v_s) and CH-bending (quantum number v_b) states such as

$$|v_s, v_b = 0\rangle, |v_s - 1, 2\rangle, |v_s - 2, 4\rangle, \dots .$$

These states have fairly similar energies, because the bending fundamental is at 1362 cm^{-1}, about half the wave number of the stretching fundamental at 2991 cm^{-1}. The multiplets of states can be characterized by a common chromophore quantum number

$$N = v_s + \tfrac{1}{2}v_b. \tag{1}$$

Integral values of N correspond to a pure stretching overtone $|v_s\rangle$ as parent chromophore state, which carries the oscilla-

TABLE I. Dye lasers used in the photoacoustic spectroscopy.

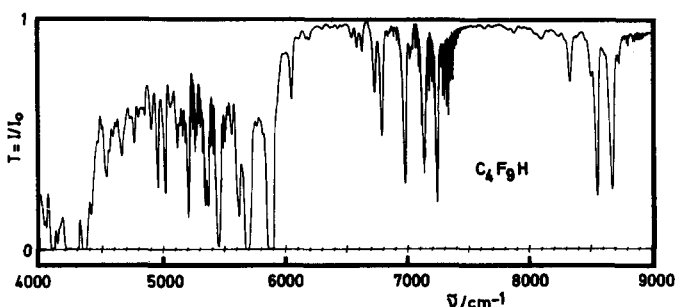| Dye	Pump laser	λ /nm	$\bar{\nu}$/cm^{-1}
LD 700	6 W, all read lines Kr$^+$laser	710 to 820	14 000 to 12 000
DCM	4 W, all visible lines Ar$^+$ laser	605 to 695	16 500 to 14 400
Rhodamine 6 G	4 W, all visible lines Ar$^+$ laser	590 to 630	17 000 to 16 000

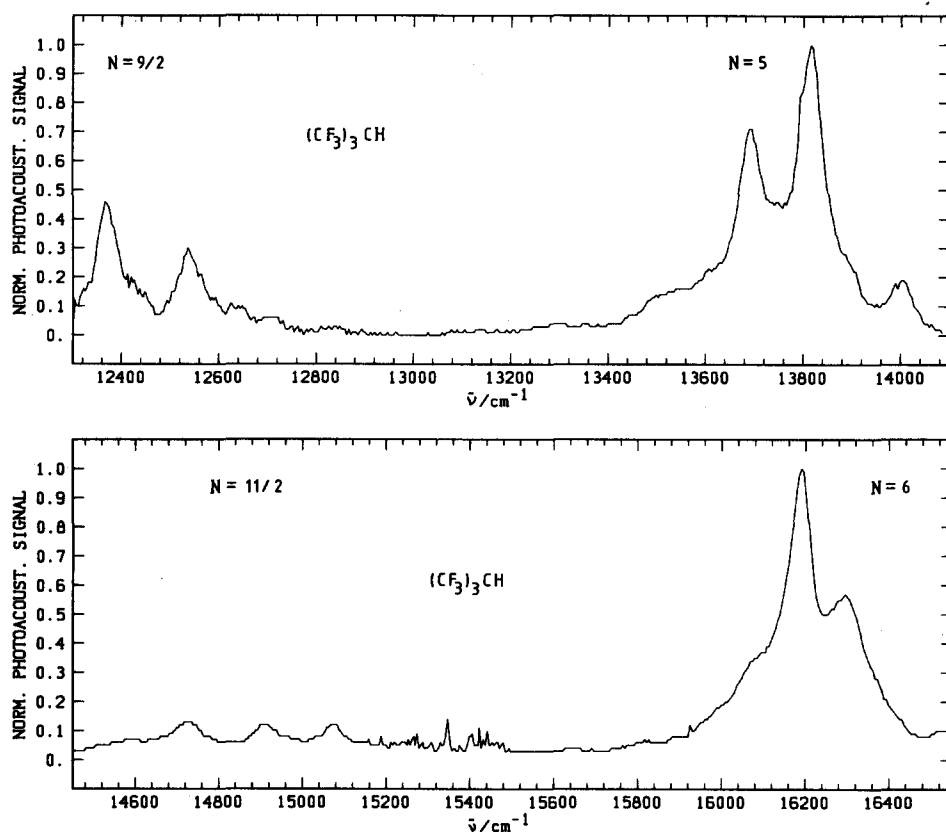FIG. 1. Survey FTIR transmission spectrum of (CF$_3$)$_3$CH (P = 4.74$\times$10^4 Pa and l = 22.5 m).

FIG. 2. Survey photoacoustic spectrum of (CF₃)₃CH between 12 300 and 16 500 cm⁻¹. The signal strengths of (a) and (b) are not directly comparable (see the text).

tor strength. Half-integral values of N correspond to a parent chromophore state with one quantum of the bending vibration in the combination $|v_s, v_b = 1\rangle$. The band system around 7000 cm⁻¹ corresponds to such a combination tone Fermi resonance polyad with $N = 5/2$. The polyads for half-integral N arise from the coupled states

$$|v_s, v_b = 1\rangle, |v_s - 1, 3\rangle, |v_s - 2, 5\rangle, \dots .$$

Bands with integral N are polarized parallel to the symmetric top axis, whereas bands with half-integral N are polarized perpendicular to the symmetric top axis. However, in contrast to small molecules, where the rotational structure and polarization is easily established, in (CF₃)₃CH the band contours are so broad that a distinction between parallel and perpendicular bands is only possible from the band contours in the region of the fundamental transitions. Our assignments are therefore based on the band positions and intensities only, in relation to the theory discussed below.

A similar multiplet pattern is repeated for the vibrational overtone spectra in the visible, which are shown in Fig. 2. The appropriate ranges are already denoted by the corresponding chromophore quantum numbers and one recognizes easily that the integrated overtone absorptions in the near IR and visible regions are essentially due to the CH chromophore. The complex structure of this absorption can be understood only from a more detailed analysis of the CH dynamics. Before we discuss this in the next section, it is necessary to outline the data treatment for the multiplets with overlapping bands (all bands above 10 000 cm⁻¹) where the band positions and widths cannot be taken directly from the raw data. This is illustrated in Fig. 3 for the remaining $N = 4$ polyad band system. For each expected vibrational

band of the CH chromophore (five for this polyad) a rotational structure was calculated and convoluted with an effectively continuous, vibrational, homogeneous, and inhomogeneous band shape of approximately Lorentzian form.[10] The rotational band structure can, to a good approximation, be described by the appropriate rigid rotor formulas[2] with the rotational constants $B \simeq 0.031\,49$ cm⁻¹ and $C \simeq 0.020\,66$ cm⁻¹ calculated from the electron diffraction structure.[16]
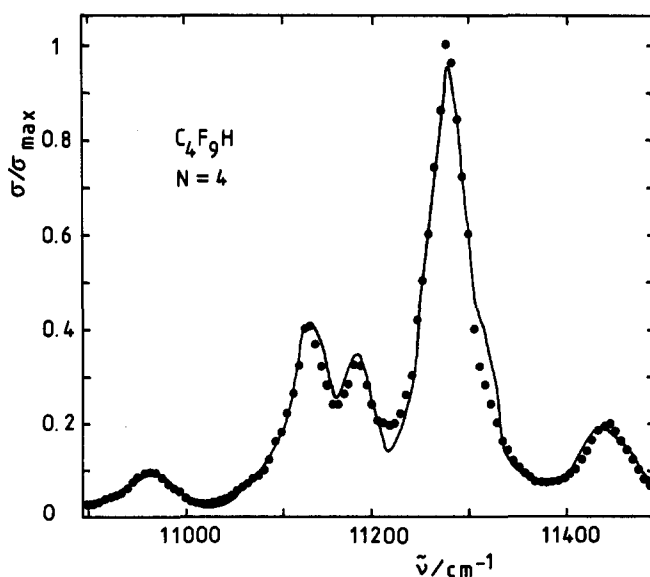

FIG. 3. FTIR spectrum (σ/σ_{max}) of (CF₃)₃CH in the range of the $N = 4$ polyad with overlapping bands. The full line is the experimental spectrum and the points are from the best fit using the deconvolution procedure described in the text.

Details of the method of band simulation with efficient algorithms for large polyatomic molecules have been described elsewhere.[10,18] The parameters in this treatment are the individual vibrational band positions, intensities, and widths. They were adjusted until a good fit was obtained (points in Fig. 3). These experimental parameters are given in the column "exp" of Tables II and III. The method of evaluation and the meaning of the vibrational widths have been discussed in more detail elsewhere[18] (see also Sec. III D).

B. Analysis of the overtone polyads with the Fermi resonance Hamiltonian

The observed spectra can be analyzed quantitatively with the general effective Fermi resonance Hamiltonian for the HCX₃ symmetric top molecules which has been discussed in detail in Ref. 8. The diagonal elements are given in cm⁻¹ units

$$H_{nn}^{N} = \tilde{\nu}'_s v_s + \tilde{\nu}'_b v_b + x'_{ss} v_s^2 + x'_{bb} v_b^2 + x'_{sb} v_s v_b + g'_{bb} l_b^2. \quad (2)$$

The $\tilde{\nu}'_i$ and x'_{ij} have their usual spectroscopic meaning. The primes indicate that a part of the anharmonic interactions of the vibrational modes are not included in the effective anharmonic constants, but are explicitly treated by the off-diagonal elements of the Hamiltonian. The vibrational angular momentum quantum number l_b is equal to zero for integral N and equal to one for half integral N; g'_{bb} is the corresponding spectroscopic constant.[2] The vibrational Hamiltonian is assumed to be approximately block diagonal in l_b and in N. Each block is a tridiagonal symmetric matrix with off-diagonal elements[8,20]

$$H_{v_s v_b l_b;(v_s - 1),(v_b + 2),l_b}^{N}$$
$$= \langle v_s, v_b, l_b | k_{sbb} q_s q_b^2 | v_s - 1, v_b + 2, l_b \rangle$$
$$= -\tfrac{1}{4} k_{sbb} \left[\tfrac{1}{2} v_s (v_b - l_b + 2)(v_b + l_b + 2) \right]^{1/2}. \quad (3)$$

TABLE II. (A) A_1 polyads—FTIR spectra and (B) A_1 polyads—photoacoustic spectra.

N	j	exp[a] $\tilde{\nu}/cm^{-1}$	Foot notes	I $\tilde{\nu}/cm^{-1}$	II $\tilde{\nu}/cm^{-1}$	Γ/cm^{-1} [e]	g(exp)[g]	I g(calc)	II g(calc)	I weight	II weight
(A)											
1	1	2 991.5	a	2 993.5	2 994.3	3.0	0.97	0.97	0.97	1	1
	2	2 705		2 704	2 702	5	0.03	0.03	0.03	1	1
2	1	5 880		5 880	5 881	11.5	0.87	0.89	0.90	0.5	1
	2	5 688		5 679	5 678	23	0.13	0.11	0.10	0.5	1
	3	...		5 389	5 386	...	...	0.002	0.002	...	
3	1	8 680		8 678	8 678	28	0.54	0.58	0.59	0.33	1
	2	8 559		8 543	8 543	16.5	0.40	0.39	0.38	0.33	1
	3	8 336		8 334	8 333	(24)	0.06	0.03	0.03	0.33	1
	4	8 060	b	8 052	8 050	...	weak	0.0003	0.0003	0.33	1
4	1	11 450	c,d	11 443	11 443	53	0.11	0.11	0.11	0.25	1
	2	11 280	c,d	11 287	11 287	44.5	0.57	0.60	0.60	0.25	1
	3	11 131	c,d	11 153	11 151	42.5	0.19	0.28	0.28	0.25	1
	4	10 965	c,d	10 956	10 956	49	0.05	0.01	0.01	0.25	1
	5	...		10 692	10 690	...	...	0.0002	0.0002	...	
(B)											
5	1	...		14 214	14 215	...	...	0.007	0.007	...	
	2	14 002	c	13 996	13 996	45.5	0.05	0.10	0.10	0.2	1
	3	13 817	c	13 824	13 824	83	0.53	0.49	0.49	0.2	1
	4	13 686	c	13 699	13 700	75	0.32	0.38	0.38	0.2	1
	5	13 526	c	13 536	13 538	98	0.08	0.02	0.02	0.2	1
	6	13 313	c	13 301	13 302	93	0.02	0.0002	0.0002	0.2	1
6	1	...		16 987	16 989	...	...	0.0003	0.0003	...	...
	2	16 722	c	16 722	16 723	126	0.08	0.006	0.006	0.167	1
	3	16 488	c	16 492	16 493	95	0.03	0.06	0.05	0.167	1
	4	16 295	c	16 301	16 302	120	0.32	0.27	0.25	0.167	1
	5	16 180	c	16 161	16 161	80	0.44	0.55	0.56	0.167	1
	6	16 066	c,f	16 053	16 057	76	0.10	0.11	0.13	0.167	1
	7	...		15 872	15 877	...	...	0.001	0.001	...	...

[a] Effective band centers at 300 K. For $N = 1$, $j = 1$ an extrapolation to 0 K yields a true vibrational fundamental frequency of 2994 cm⁻¹ (see Ref. 18).
[b] Several very weak absorptions were detected between 8000 and 8200 cm⁻¹.
[c] The data have been deconvoluted as described in the text.
[d] There is an additional component at $\tilde{\nu} = 11\,185$ cm⁻¹ with $\Gamma \simeq 23$ cm⁻¹ and $g \simeq 0.08$, due to a local resonance.
[e] Phenomenological vibrational (Lorentzian) width corrected for the rotational contribution (see the text).
[f] The deconvolution suggested an additional component at $\tilde{\nu} = 15\,991$ cm⁻¹ with $\Gamma = 68$ cm⁻¹ and $g = 0.029$.
[g] The absolute intensities $G(N) = \Sigma_{\text{polyad}} G_k$ [see Eq. (6)], i.e., integrated over all bands of one polyad N are $G(1) = 8.5 \times 10^{-3}$ (pm)²; $G(2) = 8.5 \times 10^{-4}$ (pm)²; $G(3) = 2.8 \times 10^{-5}$ (pm)²; $G(4) = 2.2 \times 10^{-6}$ (pm)²; $G(5) = 2.1 \times 10^{-7}$ (pm)²; $G(6) = 2.4 \times 10^{-8}$ (pm)²; $G(5)$ and $G(6)$ have been measured using benzene as a reference as described previously (Refs. 6 and 27).

TABLE III. (A) E polyads—FTIR spectra and (B) E polyads—photoacoustic spectra.

State		exp[a] $\tilde{\nu}$/cm^{-1}	Foot notes	I $\tilde{\nu}$/cm^{-1}	II $\tilde{\nu}$/cm^{-1}	g(exp)	I g(calc)	II g(calc)	I weight	II weight
N	j									
(A)										
1/2	1	1 362	b	1 358	1 356	= 1	1	1	2	1
3/2	1	4 352		4 345	4 342	≈0.99	0.95	0.95	0.667	1
	2	4 048		4 052	4 046	≈0.01	0.05	0.05	...	...
5/2	1	7 240		7 232	7 229	0.75	0.80	0.81	0.4	1
	2	6 980		7 015	7 011	0.25	0.19	0.19	0.4	1
	3	6 730		6 727	6 721	v. weak	0.01	0.006	...	...
7/2	1	10 048	c	10 042	10 039	...	0.45	0.45	0.286	1
	2	(9 885)	c	9 869	9 866	...	0.49	0.48	...	...
	3	9 645	c	9 655	9 651	...	0.07	0.06	0.286	1
	4	...		9 379	9 374	...	0.001	0.001	...	...
(B)										
9/2	1	12 825		12 821	12 818	0.03	0.10	0.10	0.222	1
	2	12 615		12 625	12 622	0.07	0.48	0.48	0.222	1
	3	12 536	d	12 454	12 452	0.21	0.38	0.38	...	...
		12 366	d						...	...
	4	12 195		12 258	12 256	0.34	0.04	0.04	0.222	1
	5	...		12 004	12 001	...	0.0009	0.0008	...	...
11/2	1	...		15 597	15 595	...	0.009	0.009	...	...
	2	...		15 353	15 351	...	0.11	0.10	...	...
	3	15 069		15 147	15 145	0.26	0.40	0.39	...	...
	4	14 908		14 979	14 977	0.27	0.41	0.43	...	...
	5	14 736		14 814	14 815	0.31	0.07	0.07	...	...
	6	14 611		14 597	14 597	0.16	0.001	0.001	...	...

[a] Effective band centers at 300 K.
[b] Bürger and Pawelke assigned the CH bending frequency at 1363 cm^{-1}.
[c] There are several other bands of similar strength at 9930, 9810, 9770, 9580, 9470, 9420, and 9300 cm^{-1} (very weak).
[d] This band is split by a local resonance.

When one diagonalizes each block $\mathbf{H}^N$ of $\mathbf{H}$ one obtains the eigenvalues E_j^N and the eigenvector matrix $\mathbf{Z}_N$[23]:

$$\mathbf{Z}_N^T \mathbf{H}^N \mathbf{Z}_N = \text{diag}(E_1^N,...,E_n^N). \qquad (4)$$

With strong mixing even an approximate assignment of the states by the quantum numbers v_s and v_b is impossible and we label the states by the symbol $(N)_j$ standing for the jth eigenstate of the Nth block. The quantum number j orders the eigenvalues in descending order. If only one zero order "chromophore" state $|v_s, v_b = 0, l_b = 0\rangle$ for integral N and $|v_s, v_b = 1, l_b = 1\rangle$ for half integral N has an appreciable transition moment to the ground state one can calculate the relative intensities g_j within each polyad by means of Eq. (5):

$$g_j = |Z_{1j}|^2, \qquad (5a)$$

$$\sum_j g_j = 1. \qquad (5b)$$

The corresponding experimental relative intensities (proportional to the squares of the transition moment) are defined by Eq. (6):

$$g_j(\text{exp}) = G_j / \sum_{\text{polyad}} G_k, \qquad (6a)$$

$$G_k = \int_{\text{band } k} \sigma(\tilde{\nu}) \frac{d\tilde{\nu}}{\tilde{\nu}} \cong \frac{1}{\tilde{\nu}_0 cl} \int_{\text{band } k} \ln \frac{I_0}{I} d\tilde{\nu} \qquad (6b)$$

with the usual definitions for the absorption cross section σ, the band center $\tilde{\nu}_0$, concentration c, optical path length l, incident (I_0), and transmitted (I) intensities. The seven theoretical model parameters in Eqs. (2) and (3) were adjusted in least squares fits[24] to the experimental data for 31 bands with significant positions and intensities. Two fits were used. In one fit (II) equal weight was given to all band frequencies, whereas in the more realistic fit (I) the weight was estimated according to the accuracy of the data, which decreases with increasing wave number (the weight is taken to be proportional to N^{-1}). The weights are given in the last columns of Tables II and III. The relative band intensities have been used as a check. The best fit parameters of the Hamiltonian are summarized in Table IV. The differences of the results for the two fits give an indication, to what extent the parameters of the Hamiltonian are well determined. The relative accuracy is seen to be good for all parameters except x'_{bb} and g'_{bb}, whose absolute magnitudes are too small for a precise determination. An analysis of the sensitivity of the results to a variation in x'_{sb} indicate a somewhat larger possible range ($\pm$ 5 cm^{-1}) than would appear just from Table IV. The root–mean–square deviation of the fits is, of course, much larger than for the high resolution data of CD₃H and CF₃H. However, in view of the broad bands and the very large fre-

TABLE IV. Parameters of the Fermi resonance Hamiltonian.

	Fit I[a]	Fit II[b]
$\tilde{v}_s'/\text{cm}^{-1}$	3042.8	3044.1
$\tilde{v}_b'/\text{cm}^{-1}$	1356.4	1355.1
x_{ss}'/cm^{-1}	− 56.9	− 57.2
x_{sb}'/cm^{-1}	− 14.0	− 13.5
x_{bb}'/cm^{-1}	− 0.32	− 0.23
g_{bb}'/cm^{-1}	+ 1.55	− 1.60
k_{sbb}/cm^{-1}	(±)65.5[c]	(±)65.1[c]

[a] Data weighted with N^{-1}, root–mean–square deviation 11.3 cm⁻¹.
[b] All data given equal weight, root–mean–square deviation 11.2 cm⁻¹.
[c] The sign is not directly available from experiment (see the text).

quency ranges covered by the data, there is essentially excellent agreement between experiment and the model. The agreement can also be judged by comparing in detail the relevant columns in Tables II and III. An even better visualization is given in Fig. 4, where we have drawn for the $N = 5$ and $N = 6$ polyads the experimental spectra and the corresponding theoretical stick spectra indicating both vibrational band positions and intensities. Essentially the same theoretical predictions for the high overtone spectra result, if the parameters of the Hamiltonian are derived from the FTIR data alone. In fact, such predictions were made by the Zürich group[14] before the visible spectra were measured by the Stanford group. This predictive power of the model gives us
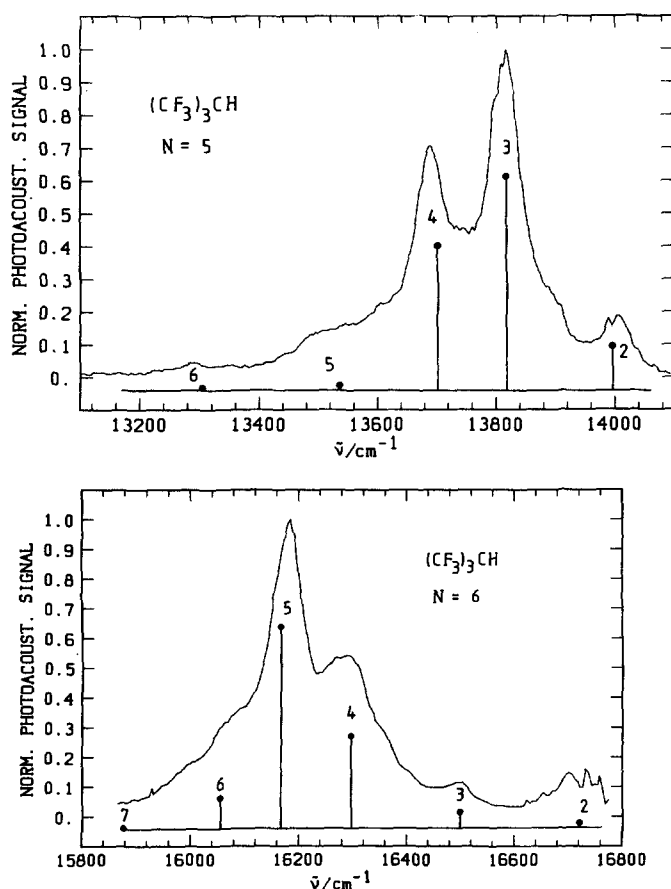
confidence that the effective Hamiltonian thus derived gives an adequate description of the short time (large energy) dynamics of the CH stretching and bending vibrations for energies as high as 17 000 cm⁻¹ in (CF₃)₃CH.

Among the more notable differences between the experiment and the model prediction one should mention the additional splitting in the $N = 4$ band system, which is certainly due to a local resonance of unknown origin, and the more pronounced, systematic discrepancies for the $N = 9/2$ and $N = 11/2$ perpendicular band systems. For these weaker combination bands the "background absorption" from combinations with other vibrations might contribute. The systematic trend with increasing energy suggests, however, a less trivial explanation. For these high energies the classical bending amplitude is calculated to be more than 45° off the symmetry axis.[9] At these large amplitudes there will be appreciable interaction with the bulky CF₃ groups. This interaction will lead at some point to a failure of the model Hamiltonian, clearly depending upon the vibrational angular momentum of the hydrogen atom around the symmetry axis. In order to account for this, additional terms in the Hamiltonian should be included for the anisotropy of the angular potential, but the experimental data are insufficient to justify this. The effect deserves further study in other cases. In the present example the explanation must remain speculative. The possible role of the neglected interpolyad couplings should be mentioned here, too.[8]

In order to provide a more instructive view of the energies involved in the interacting CH stretching and bending manifolds, Fig. 5 shows the zero order energies $[H_{nn}^N, \text{Eq.(2)}]$ plotted as the energy difference ΔE^0 from the chromophore state $|v_s,0,0\rangle$ which has zero energy by definition for each N (dashed line). For small N the pure stretching state is highest in energy. However, as the total energy increases with N, because of the large stretching anharmoni-

FIG. 4. Experimental (lines) photoacoustic spectra of the (a) $N = 5$ and (b) $N = 6$ polyad in (CF₃)₃CH, compared to theoretical stick spectra indicating the vibrational band positions and intensities.
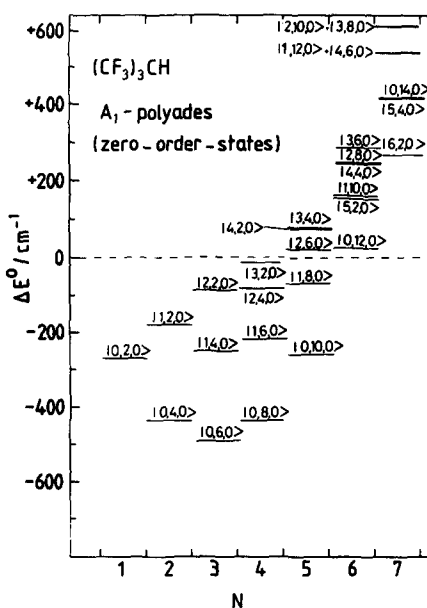

FIG. 5. Reduced zero-order energies for the A_1 polyads of the CH-stretching and bending states as a function of the chromophore quantum number N (see the detailed explanation in the text).

city and small bending anharmonicity, some zero order states with large bending excitation become higher in energy at $N = 4$. From $N = 7$ onwards the pure stretching state is lowest in energy. The figure also illustrates another point. For $N = 6$ one has a close degeneracy between $|6,0,0\rangle$ and $|10,12,0\rangle$. The direct coupling between these two states is expected to be quite small, as it corresponds to a very high term in the potential expansion. However, efficient coupling and essentially complete redistribution between stretching and bending excitation occurs via the tridiagonal chain of couplings $|6,0,0\rangle\leftrightarrow|5,2,0\rangle\leftrightarrow|4,4,0\rangle\leftrightarrow|3,6,0\rangle\leftrightarrow|2,8,0\rangle\leftrightarrow$ $|1,10,0\rangle\leftrightarrow|0,12,0\rangle$.

Figure 6 shows a survey of predicted intensity distributions in stick spectra covering the A_1 polyads from $N = 1$ to $N = 8$. As was also obvious from the experiments, there is a multitude of intense bands spread over a wide frequency range. This phenomenon is not due to "accidental" resonances occurring just for some bands in (CF₃)₃CH but it is a universal property of the isolated alkyl CH chromophore. It is also expected to occur in a similar but more complicated fashion for several coupled alkyl CH chromophores and has thus considerable importance also for the interpretation of the overtone spectra of alkane derivatives in terms of local CH-stretching modes.[13,21] We shall return to this point in Sec. III D, after a discussion of the short time evolution connected with such band systems and the underlying Hamiltonians.

C. Effective Hamiltonian and short time vibrational dynamics

The effective Hamiltonian of Eqs. (2) and (3) together with the experimental parameters of Table IV allows us to calculate the short time vibrational dynamics in the basis $|v_s,v_b,l_b\rangle$ of stretching and bending states. On somewhat
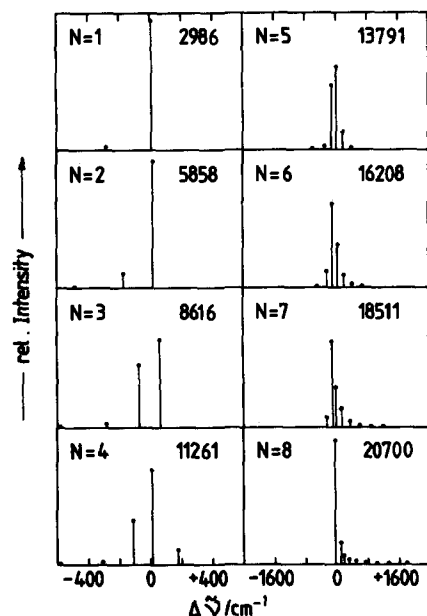

FIG. 6. Predicted coarse structures for the A_1-vibrational polyads of the CH chromophore for the quantum numbers $N = 1$ to $N = 8$. The inserted numbers indicate the zero wave number for each band, the abscissa giving the displacement from this zero, which thus corresponds to energy of the $|v_s,0,0\rangle$ state.

longer time scales the smaller interactions must be included, which lead to the "widths" of the coarse structure. Although these widths are appreciable for the higher overtones, it is instructive to consider at present just the local stretching and bending time evolution. For each block of H it can be computed with the corresponding time evolution matrix

$$U(t) = \exp(-2\pi iHt/h). \tag{7}$$

U solves the time-dependent Schrödinger equation for the amplitude vector b, the Liouville–von Neumann equation for the density matrix P or the Heisenberg equation of motion for the matrix representation Q of any observable in the basis $|v_s,v_b,l_b\rangle$:

$$b(t) = U(t)b(0), \tag{8a}$$

$$P(t) = U(t)P(0)U^\dagger(t), \tag{8b}$$

$$Q(t) = U^\dagger(t)Q(0)U(t), \tag{8c}$$

As an example, Fig. 7 shows the time evolution of the populations P_{kk} when initially the state $|v_s = 6, v_b = 0, l_b = 0\rangle$ (labeled 1) is populated. One finds a rapid decay of this state within about 0.1 ps and some subsequent oscillations. The states $|5,2,0\rangle$ (labeled 2), and $|0,12,0\rangle$ (labeled 7) are also shown. Figure 7 demonstrates that there is appreciable probability to transfer all the vibrational energy from stretching to bending excitation. Although the dominance of the initially excited pure stretching state in the oscillatory evolution on the short time scales is visible, the oscillations in the populations of all other states (2–7) look fairly irregular and in this sense similar. This can be interpreted as a first indication of a transition of statistical behavior.[22]

It should be clear that the populations in Fig. 7, although derived from experiment, have model character, because on the same or just slightly longer time scales the coupling to other vibrations will be important. From the smooth band shapes and from our work on the decay in the fundamental transitions[10,18] it can be estimated that in general there will be an approximately exponential decay of all the populations in Fig. 7, superimposed upon the oscillations. The functions given in Fig. 7. could then still be interpreted as relative populations within the CH-stretching and bend-
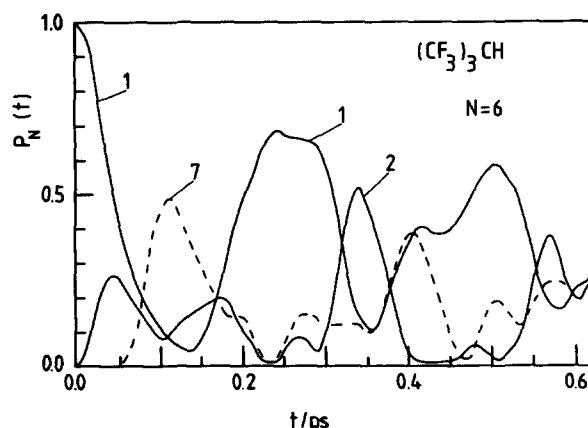

FIG. 7. Time dependent populations of some vibrational states $|v_s,v_b,l_b\rangle$ with $|6,0,0\rangle$ initially populated (labeled 1). The label 2 refers to $|5,2,0\rangle$ and 7 refers to $|0,12,0\rangle$.

ing manifolds. *The time constant of the exponential decay cannot, however, be directly determined from the observed widths because of their complex origin.*

D. Band shapes and long time evolution

The spectra of all bands including the fundamentals show smooth, broad band envelopes of widths much larger than the widths of the instrument functions which in all cases can be neglected. For the FTIR spectra the experimental resolution would have been sufficient to see rotational J structure, if there were any. The disappearance of such structure is related to the vibrational congestion which is both homogeneous and inhomogeneous.[7,10,18] The broad band shapes shown in the experimental examples have thus three contributions to their widths: (i) rotational structure, (ii) inhomogeneous (e.g., hot band) vibrational structure, and (iii) homogeneous (e.g., resonance interaction) vibrational structure. Because of the fairly weak interaction of rotation and vibration, the rotational contribution can be accounted for by an appropriate band simulation.[18] When this is done, one can extract from the experimental spectra the phenomenological widths Γ (see Table II) which are free of any rotational contribution but contain both homogeneous and inhomogeneous vibrational contributions. The difficulty in the dynamical interpretation of the widths is related to the very different dynamical significance of the two kinds of vibrational widths. Although in optical coherent experiments both widths can be related to decay phenomena, only the homogeneous widths can be associated with the decay of the population for an initially prepared CH-stretching and bending state (by energy conservation more complicated motions of the (CF₃)₃C frame are excited in this intramolecular decay).

A quantitative analysis of the homogeneous and inhomogeneous contributions has so far been possible approximately only for the fundamental transition, where the homogeneous width Γ_0 was found to be about 1 cm⁻¹ from the extrapolation of temperature-dependent spectra to 0 K.[10,18] This should be compared to the phenomenological vibrational width of 3 cm⁻¹ at 300 K. For the overtones a strong although qualitative argument concerning the homogeneous contribution can be presented as follows: From models of inhomogeneous vibrational structure one finds invariably that the inhomogeneous width should increase about linearly with the vibrational quantum number v. Any large deviation from this proves a substantial homogeneous contribution. Thus, even if the total width $\Gamma = 3$ cm⁻¹ for the fundamental were entirely inhomogeneous, the much more than linear increase of Γ with v indicates a substantial homogeneous contribution to the widths of the overtones. Rough estimates for $\Gamma_{hom}(N)$ are between $\Gamma_{hom} = 7$ cm⁻¹ for the $N = 2$ polyad and $\Gamma_{hom} = 70$ cm⁻¹ for the $N = 6$ polyad. These widths might be related to decay times $\tau = 1/(2\pi c \Gamma)$ which range between 0.8 and 0.08 ps. Although the qualitative argument concerning a large homogeneous contribution is correct, it cannot be easily made quantitative, because the homogeneous and inhomogeneous contributions to the vibrational widths are not simply additive.[18] We note also that within the polyads there are experimentally significant differences of the Γ values. A deficiency in any interpretation of the widths is our lack of knowledge about the nature of the structure underlying the widths. Therefore, although we might speculate about the decay phenomena occurring on the subpicosecond time scale, the nature of this decay, for instance which states are populated at longer times, is quite uncertain and could be derived at present only from models. Although we have developed such models in order to describe the N dependence of the widths and the relative widths within each polyad, we shall mention here only one result that seems to be largely independent of the particular model used. This concerns the fact that apparently all states $|v_s, v_b, l_b\rangle$ have some direct coupling to other molecular states, i.e., the states with large values for v_b are not the exclusive doorway states for intramolecular relaxation processes, if there are any.

It may be of interest to compare the widths found here for (CF₃)₃CH with the phenomenological widths in the CH-overtone spectra of benzene which were investigated by Bray and Berry.[12] In the case of benzene and various of its derivatives unstructured Lorentzians with widths of about 100 cm⁻¹ were observed in the overtones $v = 5$ to $v = 7$. Several theoretical interpretations in terms of intramolecular redistribution have been advanced[11,12,25–27] including also a negative result.[26] Although most models are plausible, the recent one by Sibert, Reinhardt, and Hynes[11] is particularly attractive from the present point of view. These authors have suggested that underlying the large widths in benzene overtones there is a Fermi resonance structure, which might also explain the narrowing phenomena.[27] Although it would appear from the data shown in Ref. 27 and also from independent work on C₆F₅H[28] that there are some structures which might be related to the CH-stretch, CH-bend Fermi resonance, in no case has an assignment been previously possible. In general, all structure in the high benzene overtones is washed out by the very large widths of the bands. Clearly, the dynamics of CH attached to the aromatic ring is different from the alkyl CH. Nevertheless, our results also may be of qualitative interest for interpreting the overtone spectra of benzene and its derivatives, as we have been able for the first time to resolve, identify, and assign unambiguously the dynamically important Fermi resonance of the alkyl CH chromophore in a large polyatomic molecule. A major step forward in the future would be the assignment of *further structure* underlying the quasi continuous widths in the overtones of the CH chromophore.

IV. CONCLUSIONS

(i) The isolated CH chromophore in (CF₃)₃CH, which carries oscillator strength for high overtone quantum numbers, gives us a spectroscopic window on the CH dynamics up to about half the bond dissociation energy, corresponding to classical bending amplitudes of more than ± 45°.

(ii) Instead of single bands in the overtone spectra which might be naively expected from an isolated, "local" CH-stretching mode, a complex multiplet structure is observed. The interpretation of this structure by means of the effective tridiagonal Fermi resonance Hamiltonian for the strongly

interacting CH-stretching and bending motions is established beyond doubt because of the adequate quantitative model predictions for both band positions and intensities for numerous (39) bands observed over a very large frequency range. Comparison with other alkyl CH-chromophore spectra shows, that this strong coupling of CH-stretching and bending motion is a universal phenomenon in these systems, with reasonably similar and thus transferable effective Hamiltonians.[8,9] The Fermi resonances are therefore expected to occur also in a more complicated fashion for CH$_2$ and CH$_3$ groups in large polyatomic molecules. This should lead to caution in the assignment of multiplets of bands as arising from conformers in alkanes, unless this assignment is established by isotope labeling.[21]

(iii) The time-dependent redistribution of vibrational energy between CH–stretching and bending motions on the time scale of 0.1 ps has been derived from this Hamiltonian.

(iv) The observed bands are broad, showing no detailed rotational fine structure, even at sufficiently high resolution. The widths of these bands arise largely from vibrational congestion which is both of inhomogeneous and homogeneous origin. From the much more than linear increase of these widths with the overtone quantum number, one can conclude that a substantial fraction of the vibrational overtone widths is homogeneous, corresponding to an exponential decay of the CH-stretching and bending excitation on the sub-picosecond time scale for the overtones (but more than 1 ps for the fundamental[7,18]). The nature of this decay in terms of populated final states remains conjectural.

ACKNOWLEDGMENTS

[1]Faraday Discuss. Chem. Soc. **75**, 1 (1983).

[2]G. Herzberg, *Molecular Spectra and Molecular Structure* (Van Nostrand, New York, 1945, 1966), Vols. II and III.

[3]M. Quack and J. Troe, Int. Rev. Phys. Chem. **1**, 97 (1981).

[4]S. A. Rice in *Excited States*, edited by E. C. Lim (Academic, New York, 1975).

[5]M. Quack, Adv. Chem. Phys. **50**, 395 (1982).

[6]M. -C. Chuang, J. E. Baggott, D. W. Chandler, W. E. Farneth, and Richard N. Zare, Faraday Discuss. Chem. Soc. **75**, 301 (1983).

[7]H. R. Dübal and M. Quack, Chem. Phys. Lett. **72**, 342 (1980); **80**, 439 (1981).

[8]H. R. Dübal and M. Quack, J. Chem. Phys. **81**, 3779 (1984).

[9]S. Peyerimhoff, M. Lewerenz, and M. Quack, Chem. Phys. Lett. **109**, 563 (1984).

[10]K. von Puttkamer, H. R. Dübal, and M. Quack, Faraday Discuss. Chem. Soc. **75**, 197 (1983).

[11]E. L. Sibert, W. P. Reinhardt, and J. T. Hynes, Chem. Phys. Lett. **92**, 455 (1982).

[12]R. G. Bray and M. J. Berry, J. Chem. Phys. **71**, 4909 (1979).

[13]K. Rumpf and R. Mecke, Z. Phys. Chem. B **44**, 299 (1939); B. R. Henry and W. Siebrand, J. Chem. Phys. **49**, 5369 (1968).

[14]K. von Puttkamer, H. R. Dübal, and M. Quack, Faraday Discuss. Chem. Soc. **75**, 263 (1983).

[15]D. W. Chandler, W. E. Farneth, and R. N. Zare, J. Chem. Phys. **77**, 4447 (1982).

[16]R. Stolevik and E. Thom, Acta Chem. Scand. **25**, 3205 (1971).

[17]H. Bürger and G. Pawelke, Spectrochim. Acta Part A, **35**, 565 (1979).

[18]H. R. Dübal and M. Quack (to be published).

[19]S. Andreades, J. Am. Chem. Soc. **86**, 2003 (1964) and further references quoted there; see also D. W. Weiblen, in *Fluorine Chemistry*, edited by J. H. Simons (New York, 1954), Vol. II.

[20]P. Barchewitz, *Spectroscopie Infrarouge* (Gauthiers Villars, Paris, 1961), Vol I.

[21]J. S. Wong, R. A. MacPhail, C. B. Moore, and H. L. Strauss, J. Chem. Phys. **86**, 1478 (1982).

[22]M. Quack, Faraday Discuss. Chem. Soc. **71**, 359 (1981).

[23]J. H. Wilkinson and C. Reinsch, *Handbook for Automatic Computation* (Springer, Berlin, 1971), Vol. 2.

[24]D. W. Marquardt, J. Soc. Ind. Appl. Math. **11**, 431 (1963).

[25]D. F. Heller and S. Mukamel, J. Chem. Phys. **70**, 463 (1979).

[26]P. J. Nagy and W. L. Hase, Chem. Phys. Lett. **54**, 73 (1978); **58**, 482 (1978).

[27]K. V. Reddy, D. F. Heller, and M. J. Berry, J. Chem. Phys. **76**, 2814 (1982).

[28]H. R. Dübal and M. Quack (to be published); see also Ref. 29.

[29]M. Quack, in *Energy Storage and Redistribution in Molecules*, edited by J. Hinze (Plenum, New York, 1983), p. 493.